Crossover Scaling in Dendritic Evolution at Low Undercooling

Nikolas Provatas,[1,2] Nigel Goldenfeld,[1] and Jonathan Dantzig[2]
[1]*Department of Physics, University of Illinois at Urbana-Champaign, 1110 West Green Street, Urbana, Illinois 61801*
[2]*Department of Mechanical and Industrial Engineering, University of Illinois at Urbana-Champaign, 1206 West Green Street, Urbana, Illinois 61801*

Jeffrey C. LaCombe,[3] Afina Lupulescu,[3] Matthew B. Koss,[3] and Martin E. Glicksman[3]
[3]*Rensselaer Polytechnic Institute, 110 8th Street, Troy, New York 12180-3590*

Robert Almgren[4]
[4]*Department of Mathematics, University of Chicago, Chicago, Illinois 60637*
(Received 10 November 1998)

We examine scaling in two-dimensional simulations of dendritic growth at low undercooling, as well as in three-dimensional pivalic acid dendrites grown on NASA's USMP-4 isothermal dendritic growth experiment. We report new results on self-affine evolution in both the experiments and simulations. We find that the time-dependent scaling of our low undercooling simulations displays a crossover scaling from a regime different than that characterizing Laplacian growth to steady-state growth. [S0031-9007(99)09307-2]

PACS numbers: 68.70.+w, 05.70.Ln, 64.70.Dv, 81.30.Fb

Recent computational and experimental advances in dendritic growth offer a realistic prospect for a first principles understanding of solidification microstructure formation. Early experiments [1,2] by Glicksman and co-workers on succinonitrile (SCN) provided the first benchmarks for theoretical models of dendritic growth. Comparison of experiments with theory has been difficult, however, since experiments were influenced by convection effects and performed at low undercooling using materials with low anisotropy, parameters for which computation is difficult. Such calculations can nevertheless be performed in two dimensions (2D) with state-of-the-art numerical methods combining so-called phase-field models [3–13] and adaptive-mesh refinement [14–16]. In the most recent round of experiments [17,18] Glicksman and co-workers have reported observations on pivalic acid (PVA), whose higher anisotropy brings the benchmarks closer to the parameter range of theoretical computations.

Predicting dendritic growth theoretically has focused on the tip speed and shape in the steady state. Simulations in 2D by Karma and Rappel [19] and subsequently ourselves [15] have convincingly shown that the dynamically selected steady state is indeed the fastest of the discrete set of allowed needle crystals, as predicted by solvability theory [20–24]. However, at low undercoolings the diffusion length is so large that the time needed for each dendritic arm of a growing crystal to be in isolation from the others becomes much longer than any realistic simulation time [15]. This regime, where dendrite arms cannot simply translate at a uniform speed because of their mutual interactions, was first systematically analyzed by Almgren *et al.* [25], who used solvability theory to explore the case when the temperature field strictly obeys Laplace's equation, with constant flux, at each time. They demonstrated that the dendrite tip position grows with the $3/5$ power of time, whereas the width grows with the $2/5$ power, results which were consistent with subsequent experiments in Hele-Shaw flow [26].

In this Letter we explore dendritic growth dynamics at low undercooling, using the full diffusion equation dynamics. We find that the time-dependent evolution of 2D dendrite profiles is self-affine in time, generalizing the results of Ref. [27] for the case of growth with a nonconstant flux. Underlying this scaling behavior is a power law dependence on time of the dendrite tip position and maximum dendrite width. We find that scaling of these quantities displays a crossover from a growth regime different from that of Hele-Shaw flow to one characterized by steady-state tip growth. Meanwhile, comparison of our low undercooling simulations with microscopic solvability theory gives good agreement for the value of the so-called stability parameter. We also examine scaling in 3D dendrite data on pivalic acid obtained from NASA's USMP-4 isothermal dendritic growth experiment (IDGE), also finding self-affine scaling in the global time-dependent PVA dendrite profiles.

The simulated dendrites are modeled using the phase-field model employed in [19]. Temperature T is rescaled to $U = c_P(T - T_M)/L$, where c_P is the specific heat at constant pressure, L is the latent heat of fusion, and T_M is the melting temperature. The order parameter is defined by ϕ, with $\phi = 1$ in the solid, and $\phi = -1$ in the liquid, and the interface defined by $\phi = 0$. In what follows time is rescaled by the time scale τ_0 characterizing atomic movement in the interface, and length by the length scale W_0 characterizing the width of the liquid-solid interface. The model is given by

 0031-9007/99/82(22)/4496(4)$15.00

$$\frac{\partial U}{dt} = D\nabla^2 U + \frac{1}{2}\frac{\partial \phi}{\partial t}$$
$$A^2(\vec{n})\frac{\partial \phi}{dt} = \nabla\cdot[A^2(\vec{n})\nabla\phi] + [\phi - \lambda U(1-\phi^2)](1-\phi^2) + \frac{\partial}{\partial x}\left(|\nabla\phi|^2 A(\vec{n})\frac{\partial A(\vec{n})}{\partial \phi_{,x}}\right) + \frac{\partial}{\partial y}\left(|\nabla\phi|^2 A(\vec{n})\frac{\partial A(\vec{n})}{\partial \phi_{,y}}\right), \quad (1)$$

where $D = \alpha\tau_0/W_0^2$, α is the thermal diffusivity, and λ controls the coupling of U and ϕ. Anisotropy has been introduced in Eqs. (1) by defining the width of the interface to be $W(\vec{n}) = W_0 A(\vec{n})$ and the characteristic time by $\tau(\vec{n}) = \tau_0 A^2(\vec{n})$ [19], where $A(\vec{n}) \in [0,1]$, and $A(\vec{n}) = (1-3\epsilon)[1 + \frac{4\epsilon}{1-3\epsilon}\frac{(\phi_{,x})^4+(\phi_{,y})^4}{|\nabla\phi|^4}]$. The vector $\vec{n} = (\phi_{,x}\hat{x} + \phi_{,y}\hat{y})/(\phi_{,x}^2 + \phi_{,y}^2)^{1/2}$ is the normal to the contours of ϕ, and $\phi_{,x}$ and $\phi_{,y}$ represent partial derivatives with respect to x and y. The constant ϵ parametrizes the deviation of $W(\vec{n})$ from W_0. We expect the results to be similar for other definitions of anisotropy [28]. The parameters of Eqs. (1) are related to the appropriate Stefan problem using the relationships given in [19]. In particular, W, τ, λ, and D may be chosen to simulate an arbitrary, anisotropic capillary length $d(\vec{n})$, and interface attachment coefficient $\beta(\vec{n})$, which we chosen here as $\beta = 0$, a limit appropriate for SCN and PVA.

Simulated dendrites were computed by solving Eqs. (1) using the adaptive-grid method of Refs. [15,16]. Simulated dendrites were grown in a 2D quarter-infinite space using zero-flux boundary conditions along the sides of the system. Growth was initiated by a small quarter disk of radius R_0 centered at the origin. The preferred growth directions are along the x and y axes, making these the directions of growth of dendrite branches. The order parameter is initially set to its equilibrium value $\phi_0(\vec{x}) = -\tanh[(|\vec{x}| - R_0)/\sqrt{2}]$ along the interface. The initial temperature decays exponentially from $U = 0$ at the interface to its far-field, undercooled value $-\Delta$ as $\vec{x} \to \infty$. Simulation data presented in this paper were obtained for three undercoolings: $\Delta = 0.25$, 0.1, and 0.05. Details of these data are presented in Table I. The two data sets for $\Delta = 0.1$ correspond to different minimum grid spacings $\Delta x_{\min}$ [15,16]. Seed radii used in our simulations were $R_0 = 8.5$, 15, 30, and 30 for $\Delta = 0.25$, 0.1(A), 0.1(B), and 0.05, respectively. In all cases R_0 is smaller than the thermal diffusion length by a factor of 20 or greater.

The results of our low undercooling simulations are also contrasted here with new experimental data obtained from PVA dendrites. These experiments were performed by four of the authors (LaCombe, Lupulescu, Koss and Glicksman) during NASA's USMP-4 isothermal dendritic growth experiment. This experiment is described in detail elsewhere [18]. The IDGE experiment is designed to study dendrites grown under microgravity conditions, where transport in this particular process is considered to be conduction limited. The crystals are grown in an undercooled melt, controlled to within 0.001 K. Growth is monitored thermometrically, while images are obtained from two perpendicular directions using video and still cameras (electronic and film). Experimental results presented here were compared with four independent data subsets for dendrites grown at undercoolings of 0.58, 0.63, and 0.47 K. We present the results from experiments corresponding to $\Delta = 0.052$. These data were captured at times $t_1 = 42.48$, $t_2 = 62.73$, and $t_3 = 82.98$ sec after the dendrite was detected. The anisotropy for PVA was estimated at $\epsilon_{\rm PVA} = 0.025$ [29].

We found the individual primary arms of our simulated dendrites to be self-affine, beyond some transient time, at all undercoolings examined. Figure 1 shows the (Δ-dependent) scaling profile for 2D dendrites grown at $\Delta = 0.05$ and $\Delta = 0.25$, respectively. The global scaling profile is obtained by scaling the x direction by $(x - x_b)/X_{\max}$, where $X_{\max}(t)$ is the distance from the tip $x_{\rm tip}(t)$ to the base $x_b(t)$ of the dendrite arm, and the y direction by $y/Y_{\max}(t)$, where $Y_{\max}(t)$ is the maximum half-width of the lateral dimension of the primary dendrite arm. The tip and transverse directions were found to scale

TABLE I. Parameters for simulated dendrites. The time $t^* = 255\,622.4$.

Δ	ϵ	$\Delta x_{\min}$	Δt	D	d_o	L_x	L_y
0.25	0.05	0.78	0.048	13	0.043	12 800	6400
0.1(A)	0.05	0.78	0.08	13	0.043	102 400	51 200
0.1(B)	0.05	1.56	0.08	30	0.018 46	102 400	51 200
0.05($t < t^*$)	0.025	1.56	0.03	40	0.013 85	102 400	51 200
0.05($t > t^*$)	0.025	0.78	0.03	40	0.013 85	102 400	51 200

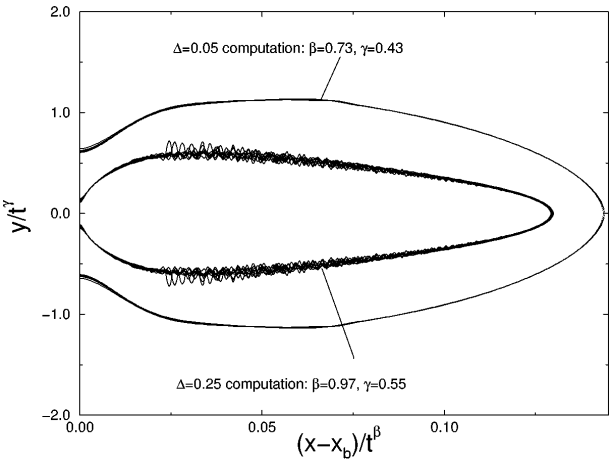

FIG. 1. Comparison of scaled dendrite profiles for $\Delta = 0.05$ and $\Delta = 0.25$. For $\Delta = 0.25$, nine times are plotted, spaced between $28\,643 < t < 66\,083$. For $\Delta = 0.05$, there are six times in the range $222\,022 < t < 279\,622$.

as $X_{\max} \sim t^{\beta}$ and $Y_{\max} \sim t^{\gamma}$, where for $\Delta = 0.05$, $0.1A$, $0.1B$, and 0.25; $\beta = 0.73$, 0.73, 0.78, and 0.97; and $\gamma = 0.43$, 0.43, 0.45, and 0.55, respectively. For the $\Delta = 0.25$ data, which at late times contained sidebranching induced by lattice noise, we define $Y_{\max}(t)$ using the *mean* interface position, obtained by smoothing the data. This definition of the sidebranch envelope gives different results than using the maximum of the sidebranch envelope [30,31].

At low undercooling, long-lived transient interactions between neighboring primary dendrite arms causes their velocity and tip radius to deviate (within simulation time scales) from their steady-state values predicted by solvability theory [15]. However, we do find that the *stability parameter* $\sigma^* = 2d_0D/VR^2$, where V and R are, respectively, the time-dependent velocity and tip radius, agrees well with the value predicted by solvability theory. Figure 2 shows σ^* vs time from our simulations at $\Delta = 0.25$, 0.1, and 0.05. Error bars were estimated using ΔV, the fluctuations in velocity, and ΔR, deviations in radius of curvature. The radius was obtained by fitting to a second order polynomial near the tip. Deviations in the fit gave an estimate for ΔR. Data for $\Delta = 0.1$ set B, omitted for clarity, converge to approximately the same σ^* as the $\Delta = 0.1$ set A data but display somewhat larger fluctuations around the mean, due to the larger grid spacing used.

The time-dependent behavior of the tip position and lateral growth rate of our 2D dendrites are characterized by the scaling of $X_{\max}(t)$ and $Y_{\max}(t)$. Figure 3 shows $X_{\max}$ and $Y_{\max}$ scaled onto respective crossover functions of the form

$$X_{\max}(t)/L_D = \frac{t}{\tau_D} F_X(t/\tau_D), \tag{2}$$

and

$$Y_{\max}(t)/L_D = \left(\frac{t}{\tau_D}\right)^{1/2} F_Y(t/\tau_D). \tag{3}$$

The parameters L_D and τ_D are effective diffusion length and time scales characterizing the intermediate regime and are fit to give collapse of the $X_{\max}$ and $Y_{\max}$ data. The data for $F_X(z)$ show a crossover scaling from fit to approximately $F_X(z) \sim z^{-0.25}$ at early times to $F_X(z) \sim z^{-0.03}$ in the steady-state regime. The crossover in $F_Y(z)$ is given by $F_Y(z) \sim z^{-0.07}$ at small z to $F_Y(z) \sim z^{0.05}$ at large arguments of $F_Y(z)$. Exponent errors were approximately ± 0.02, except for the $\Delta = 0.25$ data at late time, where they were ± 0.05. These asymptotic limits are demonstrated by the leveling off of $F_X(\chi)$ and $F_Y(\chi)$ as $\chi = t/\tau_D$ becomes large.

Our simulations are in a regime where the dendrite is much smaller than the diffusion length. However, we do not observe the early-time scaling described by Almgren *et al.* [25] since their calculations assume that dendrites are grown with a *constant* flux, whereas in our simulations the far field is diffusive with a specified small undercooling. To illustrate this difference, let us assume that the rate of change of solid fraction evolves as $F \sim t^f$, whereby the solidified area $A \sim t^{1+f}$. Since $X_{\max} \sim t^{\beta}$, $Y_{\max} \sim t^{\gamma}$, $A \sim X_{\max} Y_{\max}$, and so $1 + f = \beta + \gamma$. Since $VR^2 = \text{const}$, we obtain the scaling relation $S(f, \beta) = 4f - 5\beta + 3 = 0$. Our early-time exponents give $S(0.18, 0.75) = -0.03 \pm 0.1$. In the late-time regime, $S(0.52, 0.97) = 0.23 \pm 0.22$. The late-time error in S arises when we estimate γ by smoothing the dendrite profiles for $\Delta = 0.25$ ($\epsilon = 0.05$). For comparison, we produced data for $\Delta = 0.25$, $\epsilon = 0.025$ (not in Table I), and which were free of spurious sidebranches, obtaining $Y_{\max} \sim t^{0.5}$.

Self-affine time-dependent scaling was also found in the mean dendrite profiles of the new 3D IDGE PVA data. Figure 4 shows the scaled PVA data for $t = t_1, t_2, t_3$.

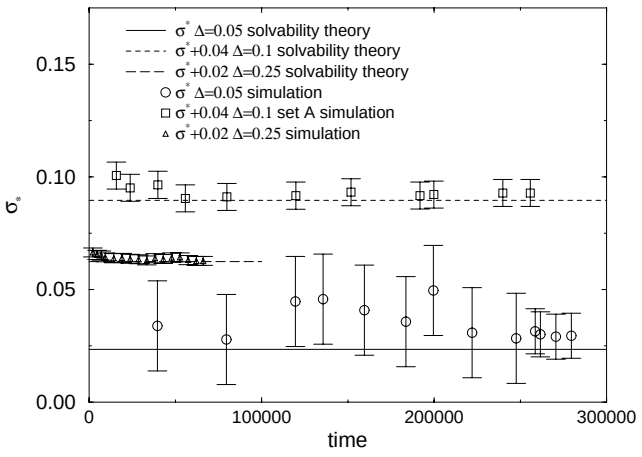

FIG. 2. Simulation data of σ^* vs time for $\Delta = 0.25$, 0.1 (set A), and 0.05. For clarity, the $\Delta = 0.1$ and 0.25 data have been shifted along the y axis by 0.04 and 0.02, respectively.

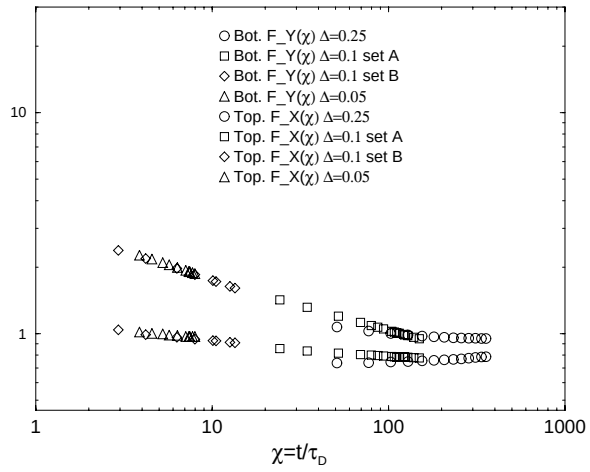

FG. 3. Crossover scaling functions describing lateral width of simulated dendrite arm $Y_{\max}$ and tip-to-base distance $X_{\max}$, for $\Delta = 0.25$, 0.1 (sets A and B), and 0.05.

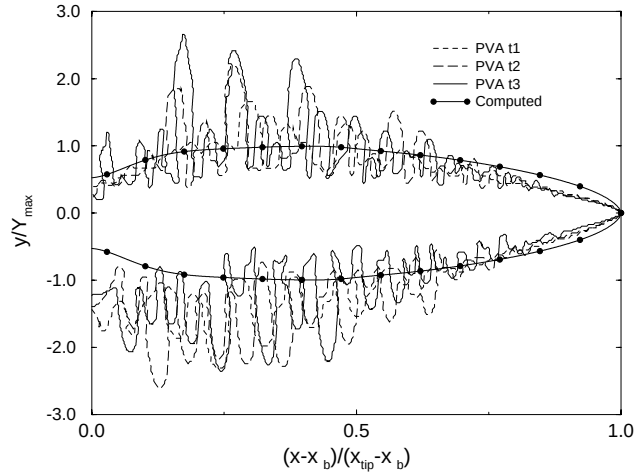

FIG. 4. Scaled USMP-4 PVA dendrites grown at $\Delta = 0.052$. 2D simulation data are superimposed for $\Delta = 0.05$, $\epsilon = 0.025$. Comparison of 2D and 3D data made merely to illustrate self-affinity in both 2D and 3D dendrites.

For comparison these data are superimposed on our 2D simulation data for $\Delta = 0.05$, $\epsilon = 0.025$. There is a slight asymmetry in the PVA data, likely due to interactions with other dendrite arms. For this reason, we scaled with respect to the top side the dendrite profile. Similar scaling was observed in all four IDGE data sets. The experimental and simulated profiles show clear differences near the tip, as one would expect. Curiously, however, the profile shapes are in good agreement away from the tip. Similar results were also found in our $\Delta = 0.1$ data. The reason for this is illustrated in Fig. 1, which shows that the difference in 2D dendrite profiles is small away from the tip.

As a plausible explanation for the apparent agreement between our low undercooling 2D simulations and our 3D experimental data, we note that away from the tip, the diffusion field is more cylindrically symmetric than at the tip because the local diffusion length is larger. Thus diffusion of heat away from the interface is better approximated by the 2D diffusion equation. We hope to examine this idea critically, as well as to accurately determine the experimental scaling behavior in future publications.

We thank Wouter-Jan Rappel for the code to obtain solvability results and Terry Chay for useful discussions. We also thank Julie Frei and Douglas Corrigan for assistance in obtaining the PVA dendrite profiles. This has been supported by the NASA Microgravity Research Program, under Grants No. NAG8-1249 and No. NAS3-25368.

[1] S.-C. Huang and M. Glicksman, Acta Metall. **29**, 1697 (1981).
[2] M. E. Glicksman, Mater. Sci. Eng. **65**, 45 (1984).
[3] J. S. Langer, *Directions in Condensed Matter* (World Scientific, Singapore, 1986), p. 164.
[4] G. Caginalp, Arch. Ration. Mech. Anal. **92**, 205 (1986).
[5] G. Caginalp, Anal. Phys. (N.Y.) **172**, 136 (1986).
[6] J. B. Collins and H. Levine, Phys. Rev. B **31**, 6119 (1985).
[7] J. A. Warren and W. J. Boettinger, Acta Metall. Mater. A **43**, 689 (1995).
[8] A. A. Wheeler, W. J. Boettinger, and G. B. McFadden, Phys. Rev. A **45**, 7424 (1992).
[9] K. R. Elder, F. Drolet, J. M. Kosterlitz, and M. Grant, Phys. Rev. Lett. **72**, 677 (1994).
[10] A. A. Wheeler, G. B. McFadden, and W. Boettinger, Proc. R. Soc. London A **452**, 495 (1996).
[11] R. Kobayashi, Physica (Amsterdam) **63D**, 410 (1993).
[12] N. Provatas, M. Grant, and K. R. Elder, Phys. Rev. B **53**, 6263 (1996).
[13] S.-L. Wang and R. F. Sekerka, Phys. Rev. E **53**, 3760 (1996).
[14] R. J. Braun and B. T. Murray, J. Cryst. Growth **174**, 41 (1997).
[15] N. Provatas, N. Goldenfeld, and J. Dantzig, Phys. Rev. Lett. **80**, 3308 (1998).
[16] N. Provatas, J. Dantzig, and N. Goldenfeld, J. Comput. Phys. **148**, 1 (1999).
[17] M. E. Glicksman, Microgravity News, NASA **4**, 4 (1997).
[18] M. B. Koss, M. E. Glicksman, A. O. Lupulescu, L. A. Tennenhouse, J. C. LaCombe, D. C. Corrigan, J. E. Frei, and D. C. Malarik, in Proceedings of the 36th Aerospace Sciences Meeting, Reno, NV, AIAA-98-0809, 1998 (unpublished).
[19] A. Karma and W.-J. Rappel, Phys. Rev. E **53**, 3017 (1995).
[20] E. Ben-Jacob, N. Goldenfeld, B. Kotliar, and J. Langer, Phys. Rev. Lett. **53**, 2110 (1984).
[21] D. A. Kessler, J. Koplik, and H. Levine, Phys. Rev. A **30**, 3161 (1984).
[22] D. A. Kessler, J. Koplik, and H. Levine, Adv. Phys. **37**, 255 (1988).
[23] E. Brener and V. I. Melnikov, Adv. Phys. **40**, 53 (1991).
[24] Y. Pomeau and M. B. Amar, *Solids far from Equilibrium*, edited by C. Godreche (Cambridge University Press, Cambridge, England, 1991), p. 365.
[25] R. Almgren, W. S. Dai, and V. Hakim, Phys. Rev. Lett. **71**, 3461 (1993).
[26] J. Ignés-Mullol and J. Maher, Phys. Rev. E **53**, 3788 (1996).
[27] R. Almgren, J. Comput. Phys. **106**, 337 (1993).
[28] G. Caginalp, IMA J. App. Math. **39**, 51 (1987).
[29] M. Muschol, D. Liu, and H. Z. Cummins, Phys. Rev. A **46**, 1038 (1992).
[30] Q. Li and C. Beckermann, Phys. Rev. E **57**, 3176 (1997).
[31] U. Bisang and J. H. Bilgram, Phys. Rev. Lett. **75**, 3898 (1995).